

J-GEM Follow-Up Observations to Search for an Optical Counterpart of The First Gravitational Wave Source GW150914

Tomoki MOROKUMA¹, Masaomi TANAKA², Yuichiro ASAKURA³, Fumio ABE³, Paul J. TRISTRAM⁴, Yousuke UTSUMI⁵, Mamoru DOI¹, Kenta FUJISAWA⁶, Ryosuke ITOH⁷, Yoichi ITOH⁸, Koji S. KAWABATA⁵, Nobuyuki KAWAI⁹, Daisuke KURODA¹⁰, Kazuya MATSUBAYASHI¹¹, Kentaro MOTOHARA¹, Katsuhiko L. MURATA¹², Takahiro NAGAYAMA¹³, Kouji OHTA¹¹, Yoshihiko SAITO⁹, Yoichi TAMURA¹, Nozomu TOMINAGA^{14,15}, Makoto UEMURA⁵, Kenshi YANAGISAWA¹⁰, Yoichi YATSU⁹ and Michitoshi YOSHIDA⁵

¹Institute of Astronomy, Graduate School of Science, University of Tokyo, 2-21-1, Osawa, Mitaka, Tokyo 181-0015, Japan

²National Astronomical Observatory of Japan, Mitaka, Tokyo 181-8588, Japan

³Institute for Space-Earth Environmental Research, Nagoya University, Chikusa-ku, Nagoya 464-8601, Japan

⁴Mt. John University Observatory, Lake Tekapo 8770, New Zealand

⁵Hiroshima Astrophysical Science Center, Hiroshima University, Hiroshima 739-8526, Japan

⁶The Research Institute of Time Studies, Yamaguchi University, Yamaguchi 753-8511, Japan

⁷Department of Physical Science, Hiroshima University, Hiroshima 739-8526, Japan

⁸Nishi-Harima Astronomical Observatory, University of Hyogo, Hyogo 679-5313, Japan

⁹Department of Physics, Tokyo Institute of Technology, Meguro-ku, Tokyo 152-8551, Japan

¹⁰Okayama Astrophysical Observatory, National Astronomical Observatory of Japan, Asakuchi, Okayama 719-0232, Japan

¹¹Department of Astronomy, Kyoto University, Kitashirakawa-Oiwake, Kyoto 606-8502, Japan

¹²Department of Particle and Astrophysical Science, Nagoya University, Chikusa-ku, Nagoya 464-8602, Japan

¹³Graduate School of Science and Engineering, Kagoshima University, Kagoshima 890-0065, Japan

¹⁴Department of Physics, Faculty of Science and Engineering, Konan University, Kobe, Hyogo 658-8501, Japan

¹⁵Kavli Institute for the Physics and Mathematics of the Universe (WPI), The University of Tokyo, Kashiwa, Chiba 277-8583, Japan

*E-mail: tmorokuma@ioa.s.u-tokyo.ac.jp

Received ; Accepted

Abstract

We present our optical follow-up observations to search for an electromagnetic counterpart of the first gravitational wave source GW150914 in the framework of the Japanese collaboration for Gravitational wave ElectroMagnetic follow-up (J-GEM), which is an observing group utilizing optical and radio telescopes in Japan, as well as those in New Zealand, China, South Africa, Chile, and Hawaii. We carried out a wide-field imaging survey with Kiso Wide Field Camera

(KWFC) on the 1.05-m Kiso Schmidt telescope in Japan and a galaxy-targeted survey with Tripole5 on the B&C 61-cm telescope in New Zealand. Approximately 24 deg^2 regions in total were surveyed in *i*-band with KWFC and 18 nearby galaxies were observed with Tripole5 in *g*-, *r*-, and *i*-bands 4-12 days after the gravitational wave detection. Median 5σ depths are $i \sim 18.9 \text{ mag}$ for the KWFC data and $g \sim 18.9 \text{ mag}$, $r \sim 18.7 \text{ mag}$, and $i \sim 18.3 \text{ mag}$ for the Tripole5 data. Probability for a counterpart to be in the observed area is 1.2% in the initial skymap and 0.1% in the final skymap. We do not find any transient source associated to an external galaxy with spatial offset from its center, which is consistent with the local supernova rate. We summarize future prospects and ongoing efforts to pin down electromagnetic counterparts of binary black hole mergers as well as neutron star mergers.

Key words: gravitational waves — black hole physics — surveys — methods: observational — binaries: close

1 Introduction

A new generation of gravitational-wave (GW) detectors, Advanced LIGO (Abbott et al. 2016a), Advanced Virgo (Acernese et al. 2015), and KAGRA (Somiya 2012), are designed to detect GWs from mergers of neutron stars (NSs) and black holes (BHs). These new detectors are much more sensitive than ever; with the design sensitivity, the horizon distance will reach $\sim 200 \text{ Mpc}$ for NS-NS mergers and a few Gpc for BH-NS or BH-BH mergers and many detections of GW events per year are expected (Abbott et al. 2016e).

Detections of electromagnetic (EM) counterparts are essential to study their astrophysical properties and environments. However, since positional localization only with the GW detectors is not accurate, which is larger than 100 deg^2 during their early observing run (Kasliwal & Nissanke 2014; Singer et al. 2014) and a few 10 deg^2 even in the LIGO-Virgo-KAGRA era (Nissanke et al. 2013; Kelley et al. 2013), it is a big challenge to identify the EM counterparts. To guide surveys for the EM identification, various kinds of EM signals have been theoretically studied over a wide wavelength range, from radio (Nakar & Piran 2011), infrared, optical, and ultraviolet (Li & Paczyński 1998; Kulkarni 2005; Metzger et al. 2010; Tanaka & Hotokezaka 2013), X-ray (Nakamura et al. 2014; Metzger & Piro 2014), and to gamma-ray (e.g., short gamma-ray burst; Metzger & Berger 2012). Consequently, we have organized a group to carry out systematic follow-up observations of GW sources using Japanese facilities called “Japanese collaboration for GW EM follow-up (J-GEM)” as part of a larger worldwide EM follow-up effort.

Recently Advanced LIGO reported the first detection of the GW event (GW150914, Abbott et al. 2016c). The signal was detected at 09:50:45 on 2015 September 14 UT, 4 days before the official start of the first observing run (O1) and an alert was delivered via GCN Notices in a machine-readable way at 03:12:12 and by an e-mail manually at 05:39:44 on 2015 September 16 UT. The waveform indicates that the source of

the GWs is a merger of two BHs, whose masses are estimated to be $36^{+5}_{-4} M_{\odot}$ and $29^{+4}_{-4} M_{\odot}$, and that the luminosity distance is $410^{+160}_{-180} \text{ Mpc}$ (The LIGO Scientific Collaboration & the Virgo Collaboration 2016). The position of the source is localized to 590 deg^2 (90 % probability). We note that, at the time of the initial alert, a classification of this GW source was not shared with the EM observers and the BH-BH nature was informed after our observations presented in this *Letter*.

To search for an EM counterpart of GW150914, extensive EM follow-up observations have been performed following the alert Abbott et al. 2016d; Abbott et al. 2016b). In this *Letter*, we report optical follow-up observations for GW150914 by the J-GEM collaboration. We refer to a skymap promptly produced with LALInference Burst (LIB; Lynch et al. 2015) as the initial skymap and to the most accurate LALInference (Veitch et al. 2015) skymap distributed on 2016 January 13 as the final skymap. All the magnitudes shown in this *Letter* are in the AB system.

2 J-GEM Observations for GW150914

J-GEM has observing facilities from radio to optical as listed in Table 1. They are nicely distributed all over the Earth in terms of the longitude of the sites. Among them, we utilized two telescopes to carry out two types of optical follow-up observations for GW150914: one is an imaging survey with a wide-field imaging camera, Kiso Wide Field Camera (KWFC; Sako et al. 2012) mounted to the 1.05-m Kiso Schmidt telescope in Japan and the other is galaxy-targeted observations of nearby potential host galaxies of the GW source with Tripole5 on the 61-cm Boller & Chivens (B&C) Telescope at the Mt. John University Observatory in New Zealand. Most of the high probability regions are in the southern hemisphere and are difficult to observe with most of our observing facilities. Subaru Hyper Suprime-Cam (HSC; Miyazaki et al. 2012), which has the widest field-of-view among 8m-class telescopes, was not available after the

alert until early October.

2.1 Kiso KWFC Observations

KWFC is a wide-field optical imaging camera on the 1.05-m Kiso Schmidt telescope. The camera consists of eight $2k \times 4k$ CCDs and the total field-of-view is $2.2 \text{ deg} \times 2.2 \text{ deg}$.

The KWFC observations were carried out on 2015 September 18, 4.4 days after the GW detection. We took 180-second exposures for five continuous field-of-views, approximately 24 deg^2 in total (Morokuma et al. 2016). The observed area is shown in Figure 1 and details of the observations are summarized in Table 2. High probability region in the skymap visible from the site during the night are almost towards the Sun and the target fields are observable only at very low elevation (high airmass: $\sec(z) > 3$, where z is the zenith distance) right before sunrise and during the astronomical twilight. Therefore, we chose the i -band filter to avoid high sky background due to the Sun as much as possible.

The total probability of the regions observed with KWFC to include the GW source was initially 1.2% but turned out to be 0.1% in the final skymap. The observed regions are partly overlapped with regions covered by Pan-STARRS (PS1; Smartt et al. 2016) and MASTER-NET (Lipunov et al. 2016)¹.

The data reduction procedure basically follows that of the supernova (SN) survey with KWFC (KISS; Morokuma et al. 2014). The 5σ limiting magnitudes are approximately 19 mag for the first four images and as shallow as 16.2 mag for the last image due to the twilight. For each of the fully reduced images, we applied an image subtraction method (*hotpants*²) with deeper archival Sloan Digital Sky Survey (SDSS) images taken several years ago as references. Then, we extract transient objects with positive fluxes (2.5σ , 5 pixel connection) in the subtracted images with *SExtractor* (Bertin & Arnouts 1996).

2.2 B&C 61-cm Tripole5 Observations

Tripole5 is an optical camera on the B&C 61cm telescope capable of taking images in $6.2 \text{ arcmin} \times 4.2 \text{ arcmin}$ field-of-view in g -, r -, and i -bands, simultaneously.

The observations are started on 2015 September 20, 6.3 days after the GW detection. We observed 18 nearby galaxies in the high probability region of the southern hemisphere as shown in Figure 1 and Table 3. Two to six 120-sec frames were taken per galaxy in g -, r -, and i -bands on 2015 September 20, 21, 24, and 26. The observed galaxies are selected from the Gravitational Wave Galaxy Catalogue (GWGC; White et al. 2011) based on the initial skymap and are closer than 100 Mpc so that an EM counterpart of an NS-NS merger could

be detected. All the galaxies observed are located within the $\sim 200 \text{ deg}^2$ of the overlapped localization region (90% confidence) of GW150914 and GW150914-GBM, detected with Gamma-ray Burst Monitor (GBM) onboard the Fermi Gamma-ray Space Telescope (Connaughton et al. 2016).

The total probabilities in the initial and final skymaps are 0.003% although the distance $d = 410^{+160}_{-180} \text{ Mpc}$ is farther than the maximum distances to the galaxies by a factor of ~ 4 . The number of the observed galaxies is about 4% of the galaxies in the GWGC catalog within the 90% probability region.

The data are reduced in a standard manner using *IRAF*. Zeropoint magnitudes in the g , r , and i -bands are determined relative to the B , R , and I -band magnitudes of objects in the USNO-B1.0 catalog (Monet et al. 2003) using the conversion equations in Fukugita et al. (1996). Medians of the 5σ limiting magnitudes are $g = 18.9 \text{ mag}$, $r = 18.7 \text{ mag}$, and $i = 18.3 \text{ mag}$. Object catalogs for the Tripole5 images are created using *SExtractor*.

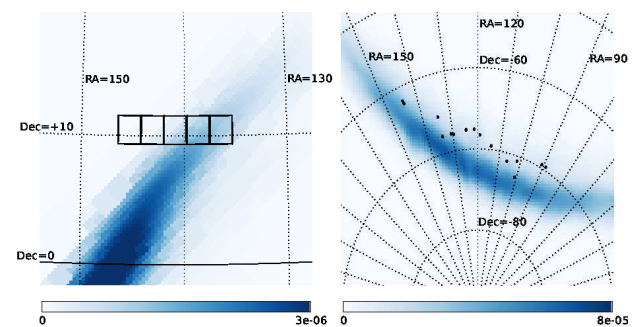


Fig. 1. Final skymap (LALInference) for the GW150914 localization and the observed regions with KWFC (left) and Tripole5 (right). The color map is shown in unit of probability per HEALPix (Górski et al. 2005) pixel of $N_{\text{side}} = 2^9 = 512$, corresponding to about 47 arcmin^2 . The KWFC field-of-views are shown in box and the area observed with Tripole5 are shown in dots.

3 Results & Discussion

For the KWFC data, radial profiles and SDSS classifications (star/galaxy separation based on *probPSF* information available in the SDSS database) of all of the transient objects are used to extract extragalactic transients. Known asteroids are also checked with *MPChecker* and removed from the transient catalog. For the Tripole5 data, the object catalog in the entire observed field of each target galaxy is first compared with the USNO-B1.0 catalog. There remain some objects without any counterparts in the USNO-B1.0 catalog and they are visually inspected by comparing the Tripole5 images with the Digitized Sky Survey images.

In these procedures described above, we find no extragalactic transient object with a spatial offset from its host galaxy although we detect variability at centers of several external galaxies (including PS15cek described below). Given the survey ar-

¹ http://master.sai.msu.ru/static/G184098/G184098_4.png

² <http://www.astro.washington.edu/users/becker/v2.0/hotpants.html>

eas, depths of the data, and the measured volumetric SN rates in the local universe (Blanc et al. 2004 for Type Ia SNe and Li et al. 2011 for Core-Collapse SNe), expected number of SNe is smaller than unity. This is consistent with the result that we do not find any SN candidate.

Among transient objects discovered and reported by other projects so far (PS1 by Smartt et al. 2016; UVOT on the Swift satellite by Evans et al. 2016; La Silla - QUEST by Rabinowitz et al. 2015, and iPTF by Singer et al. 2015 and Kasliwal et al. 2016) four transients are within the regions observed with KWFC; PS15cej, PS15cek, PS15ckf, and PS15dft (Table 4). All these PS1 transients were discovered in early October 2015, while our KWFC data were taken in September 2015. PS15cek is a known AGN (2MFGC 07447; Véron-Cetty & Véron 2001) at $z = 0.060$, and the variability is also detected in our KWFC images compared with the past SDSS data. We do not detect the other three objects, i.e., two SNe (PS15cej and PS15ckf) and one cataclysmic variable star (PS15dft or ASASSN-15se), but the non-detection of variability is not surprising since these explosions and flare are likely to occur after our observations in September (Smartt et al. 2016).

Several theoretical scenarios about EM counterparts of BH-BH mergers and their emissions are available. Nakamura et al. (2016) calculated an expected optical emission from almost the same system as GW150914. In their model, Eddington luminosity of a $60 M_{\odot}$ BH in dense interstellar medium may have brightness of about 26 mag if the emission is radiated mainly in the optical wavelength at a similar distance to GW150914 ($d \sim 300$ Mpc), which can be detected with 8m-class telescopes and instruments. Yamazaki et al. (2016) and Morsony et al. (2016) predict a wide range of EM emissions from GW150914 under an assumption that GW150914-GBM (Connaughton et al. 2016) is associated with the GW150914 (Loeb 2016). They suggest that an optical counterpart is detectable with 8-m class telescopes within 1 or a few days after the GW event and that earlier emission within several hours after the event can be detected with smaller aperture (2-4 m) telescopes.

These theoretical models indicate that wide-field surveys with 8m-class telescopes and instruments such as Subaru HSC or Large Synoptic Survey Telescope (LSST; LSST Science Collaboration et al. 2009) is the best strategy to detect an optical counterpart of a GW event like GW150914. If a similar event to GW150914 occurs at a closer distance, an optical counterpart could be detectable with 1-2-m class telescopes. Although selecting the counterpart from a huge amount of imaging data is challenging, several intensive works have been done. Implementation of machine-learning techniques for reducing real-to-bogus ratios with wide-field imaging data have been done in several projects (e.g., Bloom et al. 2012; Brink et al. 2013). Among the J-GEM instruments, machine-learning approach for effective discoveries of transient objects is being

done for Subaru HSC data (Morii et al. 2016). Effective classification trial for many transient objects (Kessler et al. 2010) by adding realistic theoretical models for GW EM counterparts including NS-NS merger (see the review by Tanaka 2016) will also help us to identify the EM counterpart in near future.

Acknowledgments

This work is supported by MEXT Grant-in-Aid for Scientific Research on Innovative Areas “New Developments in Astrophysics Through Multi-Messenger Observations of Gravitational Wave Sources” (24103003) and its Koubo Researches (25103503, 15H00788, 15H00774). This work is also supported by JSPS (15H02075). This study utilizes the archival images from the Sloan Digital Sky Survey and those from the Digitized Sky Surveys. Full acknowledgments can be found at <http://www.sdss.org/collaboration/credits.html> and <https://archive.stsci.edu/dss/acknowledging.html>, respectively.

References

- Abbott, B. P., et al. 2016a, *Physical Review Letters*, 116, 131103
- Abbott, B. P., et al. 2016b, *ArXiv e-prints*, arXiv:1602.08492
- Abbott, B. P., et al. 2016c, *Physical Review Letters*, 116, 061102
- Abbott, B. P., et al. 2016d, *ArXiv e-prints*, arXiv:1604.07864
- Abbott, B. P., et al. 2016e, *ArXiv e-prints*, arXiv:1602.03842
- Acernese, F., et al. 2015, *Classical and Quantum Gravity*, 32, 024001
- Akitaya, H., et al. 2014, *Proc. SPIE*, 9147, 914740
- Bertin, E., & Arnouts, S. 1996, *A&AS*, 117, 393
- Blanc, G., et al. 2004, *A&A*, 423, 881
- Bloom, J. S., et al. 2012, *PASP*, 124, 1175
- Brink, H., Richards, J. W., Poznanski, D., Bloom, J. S., Rice, J., Negahban, S., & Wainwright, M. 2013, *MNRAS*, 435, 1047
- Connaughton, V., et al. 2016, *ArXiv e-prints*, arXiv:1602.03920
- Evans, P. A., et al. 2016, *MNRAS*, arXiv:1602.03868
- Fukugita, M., Ichikawa, T., Gunn, J. E., Doi, M., Shimasaku, K., & Schneider, D. P. 1996, *AJ*, 111, 1748
- Górski, K. M., Hivon, E., Banday, A. J., Wandelt, B. D., Hansen, F. K., Reinecke, M., & Bartelmann, M. 2005, *ApJ*, 622, 759
- Kasliwal, M. M., & Nissanke, S. 2014, *ApJL*, 789, L5
- Kasliwal, M. M., et al. 2016, *ArXiv e-prints*, arXiv:1602.08764
- Kawabata, K. S., et al. 2008, *Proc. SPIE*, 7014, 70144L
- Kelley, L. Z., Mandel, I., & Ramirez-Ruiz, E. 2013, *Phys. Rev. D*, 87, 123004
- Kessler, R., et al. 2010, *PASP*, 122, 1415
- Konishi, M., et al. 2015, *PASJ*, 67, 4
- Kotani, T., et al. 2005, *Nuovo Cimento C Geophysics Space Physics C*, 28, 755
- Kulkarni, S. R. 2005, *arXiv:astro-ph/0510256*, arXiv:astro-ph/0510256
- Li, L.-X., & Paczyński, B. 1998, *ApJL*, 507, L59
- Li, W., Chornock, R., Leaman, J., Filippenko, A. V., Poznanski, D., Wang, X., Ganesalingam, M., & Mannucci, F. 2011, *MNRAS*, 412, 1473
- Lipunov, V., et al. 2016, *GRB Coordinates Network*, 18903
- Loeb, A. 2016, *ArXiv e-prints*, arXiv:1602.04735
- LSST Science Collaboration, et al. 2009, *ArXiv e-prints*, arXiv:0912.0201
- Lynch, R., Vitale, S., Essick, R., Katsavounidis, E., & Robinet, F. 2015, *ArXiv e-prints*, arXiv:1511.05955

- Metzger, B. D., & Berger, E. 2012, *ApJ*, 746, 48
- Metzger, B. D., & Piro, A. L. 2014, *MNRAS*, 439, 3916
- Metzger, B. D., et al. 2010, *MNRAS*, 406, 2650
- Miyazaki, S., et al. 2012, *Proc. SPIE*, 8446, 84460Z
- Monet, D. G., et al. 2003, *AJ*, 125, 984
- Morii, M., et al. 2016, submitted to *PASJ*
- Morokuma, T., et al. 2014, *PASJ*, 66, 114
- Morokuma, T., et al. 2016, *GRB Coordinates Network*, 19017
- Morsony, B. J., Workman, J. C., & Ryan, D. M. 2016, *ArXiv e-prints*, arXiv:1602.05529
- Nagashima, C., et al. 1999, in *Star Formation 1999*, ed. T. Nakamoto, 397-398
- Nagayama, T., Nagashima, C., Nakajima, Y., Nagata, T., Sato, S., Nakaya, H., Yamamuro, T., Sugitani, K., & Tamura, M. 2003, *Proc. SPIE*, 4841, 459-464
- Nakamura, T., Kashiyama, K., Nakauchi, D., Suwa, Y., Sakamoto, T., & Kawai, N. 2014, *ApJ*, 796, 13
- Nakamura, T., Nakano, H., & Tanaka, T. 2016, *ArXiv e-prints*, arXiv:1601.00356
- Nakar, E., & Piran, T. 2011, *Nature*, 478, 82
- Nissanke, S., Kasliwal, M., & Georgieva, A. 2013, *ApJ*, 767, 124
- Oshima, T., et al. 2012, in *IEEE Trans. Appl. Supercond*, Vol. 23, Ground-based and Airborne Instrumentation for Astronomy IV, 2101004-1-2101004-4
- Rabinowitz, D., Baltay, C., Ellman, N., & Nugent, P. 2015, *GRB Coordinates Network*, 18347
- Sakimoto, K., et al. 2012, *Proc. SPIE*, 8446, 844673
- Sako, S., et al. 2012, *Proc. SPIE*, 8446, 84466L
- Sako, T., et al. 2008, *Experimental Astronomy*, 22, 51
- Singer, L. P., et al. 2014, *ApJ*, 795, 105
- Singer, L. P., et al. 2015, *GRB Coordinates Network*, 18337
- Smartt, S. J., et al. 2016, *ArXiv e-prints*, arXiv:1602.04156
- Somiya, K. 2012, *Classical and Quantum Gravity*, 29, 124007
- Tanaka, M. 2016, submitted to *Advances in Astronomy*
- Tanaka, M., & Hotokezaka, K. 2013, *ApJ*, 775, 113
- The LIGO Scientific Collaboration, & the Virgo Collaboration. 2016, *ArXiv e-prints*, arXiv:1602.03840
- Veitch, J., et al. 2015, *Phys. Rev. D*, 91, 042003
- Véron-Cetty, M.-P., & Véron, P. 2001, *A&A*, 374, 92
- White, D. J., Daw, E. J., & Dhillon, V. S. 2011, *Classical and Quantum Gravity*, 28, 085016
- Yamazaki, R., Asano, K., & Ohira, Y. 2016, *ArXiv e-prints*, arXiv:1602.05050
- Yanagisawa, K., Kuroda, D., Yoshida, M., Shimizu, Y., Nagayama, S., Toda, H., Ohta, K., & Kawai, N. 2010, in *American Institute of Physics Conference Series*, Vol. 1279, American Institute of Physics Conference Series, ed. N. Kawai & S. Nagataki, 466-468
- Yanagisawa, K., et al. 2014, *Proc. SPIE*, 9147, 91476D

Table 1. J-GEM Telescopes in an order of longitude.

Site (telescope)	d [m] ^a	Location ^b	Instrument [*]	FoV	Pixel Scale ^c	Note ^f
Mt. Johns (B&C 61cm)	0.61	170.47 E, 43.40 S, 1029	Tripole5	$4'2 \times 6'2$	0.17	(1)
Mt. Johns (MOA-II)	1.8	170.47 E, 43.40 S, 1029	MOA-cam3 [1]	$1^\circ 31 \times 1^\circ 64$	0.58	(3)
Akeno (MITSuME)	0.5	138.48 E, 35.79 N, 900	(g, R_C, I_C imager)	$27'8 \times 27'8$	1.63	(1)
Kiso (Kiso Schmidt)	1.05	137.63 E, 35.79 N, 1130	KWFC [2]	$2^\circ 2 \times 2^\circ 2$	0.946	(3)
Nishi-Harima (Nayuta)	2.0	134.34 E, 35.03 N, 449	MINT	$10'9 \times 10'9$	0.32	(1)
Okayama, OAO (Kyoto-3.8m ^d)	3.8	133.60 E, 34.58 N, 343	KOOLS-IFU	$14'' \phi$	1.14	(2)
Okayama, OAO (OAO 188cm)	1.88	133.59 E, 34.58 N, 371	KOOLS-IFU	$30'' \phi$	2.34	(2)
Okayama, OAO (OAO 91cm)	0.9	133.59 E, 34.58 N, 364	OAO-WFC [3]	$28'4 \times 28'4$	1.67	(1)
Okayama, OAO (MITSuME)	0.5	133.59 E, 34.58 N, 358	(g, R_C, I_C imager) [4],[5]	$26'9 \times 26'9$	1.52	(1)
Higashi-Hiroshima (Kanata)	1.5	132.78 E, 34.38 N, 511	HOWPol [6]	$15' \phi$	0.30	(1)
Higashi-Hiroshima (Kanata)	1.5	132.78 E, 34.38 N, 511	HONIR [7],[8]	$10' \times 10'$	0.30	(1)
Yamaguchi (Yamaguchi ^e)	32×2	131.56 E, 34.22 N, 166	6-8 GHz Receiver	-	4-5 arcmin	(1)
Tibet (HinOTORI ^d)	0.5	80.03 E, 32.31 N, 5130	(u, R_C, I_C imager)	$24' \times 24'$	0.68	(1)
Sutherland, SAAO (IRSF)	1.4	20.81 E, 32.38 S, 1761	SIRIUS [9],[10]	$7'7 \times 7'7$	0.45	(1)
Pampa la Bola (ASTE ^e)	10	67.70 W, 22.97 S, 4862	ASTECAM [11]	$8'1 \phi$	20-30	(1)
Chajnantor, TAO (miniTAO)	1.04	67.74 W, 22.99 S, 5640	ANIR [12]	$5'1 \times 5'1$	0.298	(1)
Mauna Kea, MKO (Subaru)	8.2	155.48 W, 19.83 N, 4139	HSC [13]	$1^\circ 5 \phi$	0.168	(3)

References for instruments; [1]: Sako et al. (2008), [2]: Sako et al. 2012, [3]: Yanagisawa et al. (2014), [4]: Kotani et al. (2005), [5]: Yanagisawa et al. (2010), [6]:

Kawabata et al. (2008), [7]: Akitaya et al. (2014), [8]: Sakimoto et al. (2012), [9]: Nagashima et al. (1999), [10]: Nagayama et al. (2003), [11]: Oshima et al. (2012), [12]: Konishi et al. (2015), [13]: Miyazaki et al. (2012).

a: diameter of telescope primary mirror.

b: longitude and latitude in degrees, and height in meters.

c: pixel scale is in arcsec pixel⁻¹.

d: to be operated.

e: radio or submillimeter telescopes.

f: (1) galaxy-targeted; (2) integral field spectroscopy; (3) wide-field survey.

Table 2. Summary of Kiso KWFC Observations.

UT ^a	MJD ^b	Field	RA	Dec	Filter	t_{exp} ^c	$m_{\text{lim}}(5\sigma)$
2015-09-18 19:06:02	57283.7969	KT009891	09:05:35.52	+10:27:00.0	i	180	19.2
2015-09-18 19:11:37	57283.8008	KT009892	09:14:32.16	+10:27:00.0	i	180	18.9
2015-09-18 19:16:59	57283.8045	KT009893	09:23:28.80	+10:27:00.0	i	180	18.9
2015-09-18 19:22:22	57283.8083	KT009894	09:32:25.44	+10:27:00.0	i	180	18.9
2015-09-18 19:34:29	57283.8167	KT009895	09:41:22.08	+10:27:00.0	i	180	16.3

a: time starting the exposures. b: MJDs of the middle of the exposures. c: Exposure time for each field is in seconds.

Table 3. Summary of B&C 61cm telescope Tripole5 Observations.

Galaxy	RA ^a	Dec ^a	d [Mpc] ^a	Filter	2015-09-20 ^b	2015-09-21 ^b	2015-09-24 ^b	2015-09-26 ^b
ESO034-012	06:43:30.8	−72:35:41	74.22 ± 11.13	g, r, i	-	120×2	120×4	120×4
ESO058-014	06:46:36.1	−70:36:54	93.42 ± 14.01	g, r, i	-	120×2	120×4	120×4
ESO058-023	07:04:45.5	−71:00:59	92.83 ± 13.93	g, r, i	-	120×2	120×4	120×4
ESO059-023	07:56:06.1	−68:16:41	70.51 ± 10.58	g, r, i	-	120×2	120×4	120×4
ESO060-010	08:38:36.7	−67:56:11	96.96 ± 14.54	g, r, i	-	120×2	120×4	120×4
ESO060-011	08:42:43.0	−67:48:54	94.97 ± 14.25	g, r, i	120×2	120×2	120×4	120×4
ESO060-018	08:56:40.5	−67:52:13	84.89 ± 12.73	g, r, i	-	120×2	120×4	120×4
ESO089-009	08:05:09.0	−67:35:12	95.29 ± 20.96	g, r, i	120×4	120×2	120×6	120×4
ESO089-015	08:18:08.1	−67:34:37	96.53 ± 21.24	g, r, i	-	120×2	120×4	120×4
ESO089-016	08:18:23.4	−67:36:40	97.78 ± 21.51	g, r, i	120×2	120×2	120×4	120×4
ESO090-011	08:58:18.5	−65:22:03	72.93 ± 10.94	g, r, i	120×2	120×2	120×4	120×4
ESO126-023	09:37:51.2	−62:09:04	33.42 ± 5.01	g, r, i	-	120×2	120×4	120×4
ESO126-024	09:38:29.1	−61:49:47	33.42 ± 5.01	g, r, i	120×2	120×2	120×4	120×4
NGC 2150	05:55:46.3	−69:33:39	58.89 ± 8.83	g, r, i	120×3	120×2	120×4	120×4
NGC 2187	06:03:48.5	−69:35:00	59.56 ± 8.93	g, r, i	120×4	120×2	120×4	120×4
NGC 2187A	06:03:44.2	−69:35:18	50.93 ± 11.21	g, r, i	120×2	120×2	120×4	120×4
NGC 2442	07:36:23.8	−69:31:51	17.30 ± 2.60	g, r, i	-	120×3	120×4	120×4
NGC 2466	07:45:16.0	−71:24:38	70.86 ± 10.63	g, r, i	120×2	120×2	120×4	120×4

a: The coordinates of the center of the galaxy and the distances d to the galaxies are derived from the GWGC (White et al. 2011).

b: Exposure time on each date for each galaxy is in seconds.

Table 4. Transients Reported in Other Papers in Our Survey Fields.

Name	RA	Dec	Reference	Nature	Disc ^a	ID ^b	Expl. ^c	J-GEM	note
PS15cej	09:35:19.41	+10:11:50.7	Smartt et al. (2016)	SN Ia	2015-10-02	2015-10-10	2015-09-22	KWFC	before Expl.
PS15cek	09:36:41.04	+10:14:16.2	Smartt et al. (2016)	AGN	2015-10-02	-	-	KWFC	-
PS15ckf	09:45:57.71	+09:58:31.4	Smartt et al. (2016)	SN II	2015-10-03	2015-10-20	2015-09-27	KWFC	before Expl.
PS15dft	09:33:09.38	+10:28:02.2	Smartt et al. (2016)	CV	2015-10-23	-	-	KWFC	-

a: PS1 discovery date.

b: Date of PS1 spectroscopic identification.

c: Explosion date based on the spectroscopic phase.